Demonstration of a high resolution X-ray detector for medical imaging

Theodore. F. Morse^a, Nicholas Mostovych^a, Rajiv Gupta^b, Timothy Murphy^c, Peter Weber^a, Nerine Cherepy^d, Bernhard Adams^e, Thomas Bifano^f, Brian Stankus^a, Adil Akif^a Angus I. Kingon^a,

^aDept. of Engineering, Brown University, Providence, RI; ^bAXIS Center, Harvard Medical School, Boston, MA; ^cWarren Alpert Medical School of Brown University, Providence, RI; ^dLawrence Livermore National Laboratory, Livermore, CA; ^eIncom, Inc., Charlton, MA; ^fPhotonics Center, Boston University, Boston, MA

ABSTRACT

In digital X-ray imaging, a crucial factor determining image resolution of all indirect detection systems is the spread of light in the X-ray scintillator. Currently deployed clinical x-ray detectors, with a resolution between 75 and 300 microns, are affected by such spread of light. This work demonstrates the significantly improved the resolution of an indirect X-ray scintillation detector using a new structuring approach

The new structured scintillator consists of three main components: a high optical quality 'channel plate', a reflective material within the capillaries of the channel plate, and a polymer-based scintillating material that is incorporated in the capillaries. Channel plates, which are utilized for a variety of optical applications, are produced from bundles of hollow drawn borosilicate glass fibers, with repeated bundling and drawing reducing the diameter of the core and capillary pores down to values as low as 5 microns. These bundles are then cut to make high quality plates ('channel plates') with a thickness around 1 mm. Channel plates contain geometrically ordered capillary channels (about 5 million channels per square cm). The channel walls were coated with a 70 nm thick coating of Al₂O₃:W using atomic layer deposition (ALD) to optically confine the photoemission within the channel. The optical channel plates were infiltrated with a new bismuth-based scintillating polymer developed at Lawrence Livermore National Laboratory, with a photon yield of > 30,600 photons/keV for X-ray energies of 20-30 keV, a range of interest for mammography.

The new scintillator plate was used to experimentally demonstrate an X-ray resolution of 10 microns (or 50 line-pairs/mm), an approximately 7 times improvement over existing scintillating detectors. A structured scintillator plate, coupled with a digital detection system may be used to improve the spatial resolution in applications such as mammography, radiography, and computed tomography.

Keywords: indirect X-ray detectors; structured scintillators; polymer scintillators; microchannel plates; X-ray detector resolution; X-ray imaging.

1. INTRODUCTION

X-ray imaging is an invaluable tool in medicine. The aim of this research is to provide X-ray detectors with ultra-high spatial resolution approaching 5-10 microns, or 100-50 lp/mm. The spatial resolution of current systems is an order of magnitude lower than this specification. For example, current Digital Radiography (DR) plates have a spatial resolution of about 80-100 microns; traditional multidetectors (Computed Tomography) scanners have a resolution of about 200-500 microns; even the so-called microCT scanners can only deliver 20-80 micron resolution.

Applications	X-ray energy	Area (cm ²)	Spatial Resolution:
			(lp/mm): X-ray Res.
Crystallography	8-20	30x30	10:50
Mammography	20-30	20x30	15-25:75-125
Dental Imaging	50-70	2.5x3.5	7-20:35-100
NDT	30-400	>10x10	5-10:25-50
Astronomy	30-600	30x30	4-6:20-24

Table 1.1

It is well recognized that scintillator-based detector arrays have a limited resolution due to lateral spread of the photoemission within the converting layers.² This effect is highlighted in Fig. 1, showing 4π distribution. The lateral spread impacts resolution despite some crystallographic structuring in modern scintillator materials such as vapor-phase grown CsI(Tl). Significant improvements in resolution of X-ray imaging have recently been reported by fabricating silica based pores filled with CsI(Tl).^{3,4} While silica based pores filled with CsI(Tl) have demonstrated remarkable spatial resolutions down to 4 microns, these pores have only been developed to thicknesses of 40 microns which is not adequate for minimum radiographic X-ray absorption. Our research over the past few years has focused on improving the radial spread resolution issue discussed earlier by instead using optical channel plates of thicknesses sufficient for proper X-ray absorption and infiltrating the capillaries with novel polymer-based scintillator materials.^{5,6}

2. COMPONENTS AND METHODS

2.1 Polymer-based scintillator materials

The Lawrence Livermore National Laboratory has developed polymer-based scintillator materials for a variety of applications, and through a collaboration have supplied a scintillating bismuth polymer: triphenolbismuth(19%)-polyvinylcarbazol.^{7,8,9} It produces 30,640 Photons/keV, and it has a rise time of 1.2 microseconds. In can be compared to commercial CsI(Tl), which produces 55,000 Photons/keV, and it has a rise time

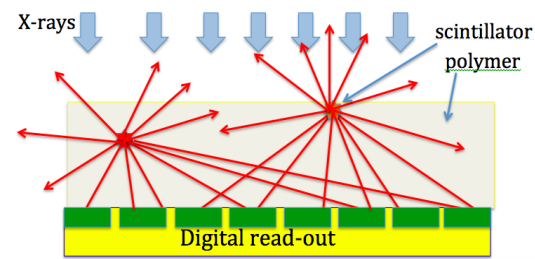


Fig. 1. A scintillator placed in front of the sensor.

of $0.98\ \mathrm{microseconds}$. The bismuth polymer developed by the Lawrence Livermore National Laboratory has

up to three times the photon flux of other "plastic" polymers.

It is worth noting that the bismuth polymer reacts to UV and wide energy X-ray radiation in a similar way. Radiation tested include soft X-rays (e.g., from synchrotron radiation), hard X-rays and Gamma rays. UV radiation is sufficiently energetic to excite electrons into the conduction band. Radiation in excess of this energy will cause scintillation. In the specific example of the bismuth polymer, the critical energy corresponds to a wavelength of 500nm.

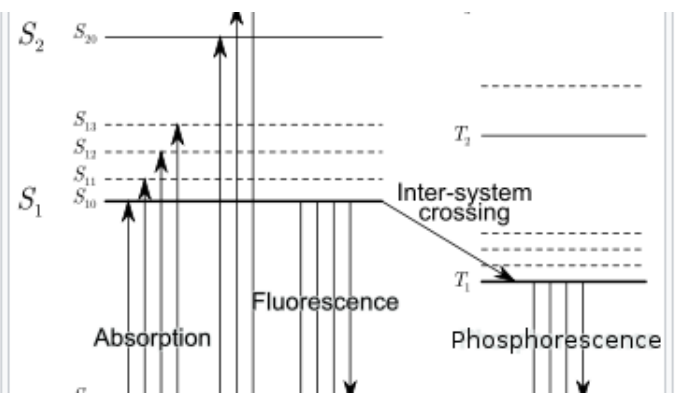


Fig. 2. Bismuth polymer subject to UV and X-Rays

2.2 Optical Channel Plates

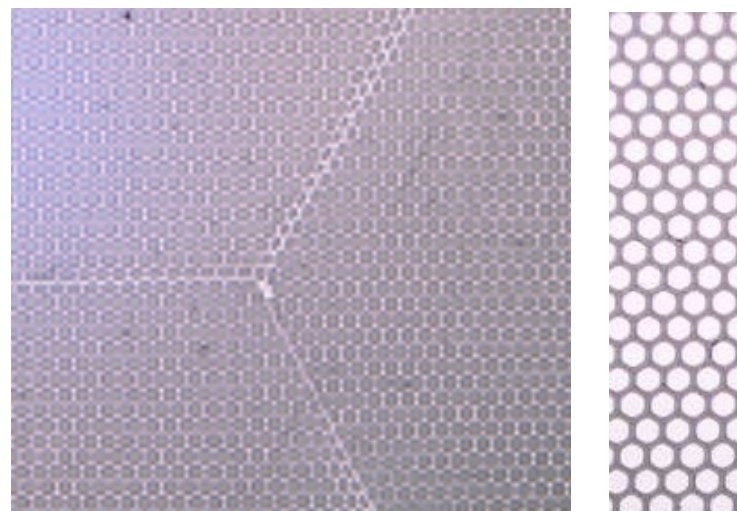
Incom, Inc. prepares optical channel plates, from coherent bundles of glass fibers in the following manner: Borosilicate glass and quartz have the remarkable property of their ductility. If a 2cm diameter hollow tube (nominally) with a 1 mm wall thickness placed in an optical fiber draw tower is heated to a sufficient temperature, and is pulled into "cane", it undergoes an affine transformation. The "cane", typically of 2 mm in length, is assembled into a "coherent bundle", that is pulled, again and again. The channel plates are cut from slices of the coherent and fused bundles of

8" x 8"	20 μ	
8" x 8"	10 μ (anticipated)	
5" x 5"	10 μ	
50mm x 53"	7 μ	
20mm x 20mm	5μ	

Table 2.

fibers. The coherent bundles that Incom makes are used for X-ray collimating devices.

The hexagonal tubes are shown in Fig. 3 and a higher magnification is shown in Fig. 4. The capillaries shown have 20,000,000 individual elements in a 20cm x 20 cm slab of cladding glass. Incom regularly produces the sizes shown in Table 2. The borosilicate glass is 25% of the total area, which leaves 75% open area to be filled with scintillating polymer.



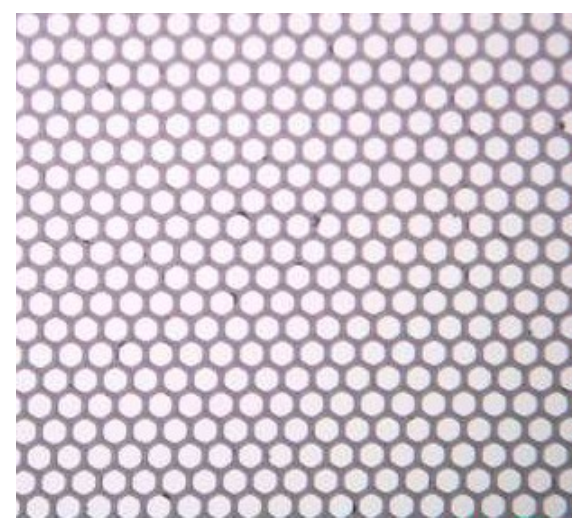


Fig. 3. 5-micron capillaries

Fig. 4. 5-micron capillary, blow-up of Fig. 3

Radiation absorption of the bismuth polymer-infiltrated optical channel plates was first tested using a 265nm UV laser. Full absorption of the UV light occurred within a few microns of the bismuth polymer through thickness.¹⁰ Total internal reflection was the means of guiding it to the sensor at the end of the fiber.

Partial absorption of 50keV X-rays was observed for a 1 mm optical channel plate infiltrated with the bismuth polymer. In addition, significant crosstalk was observed between adjacent pores demonstrating that only partial internal reflection was occurring at the pore sidewalls. In an effort to improve total internal reflection conditions in the pores, a 70nm ALD/W:Al₂O₃ layer was deposited on the pore sidewall surfaces. Increasing the reflectivity improves the critical angle of incidence for total internal reflection and drastically decreases adjacent core signal crosstalk. ¹¹ Figure 5 demonstrates qualitatively the improvement in the angle of incidence for total internal reflection inside the pores after adding the ALD/W:Al₂O₃ layer.

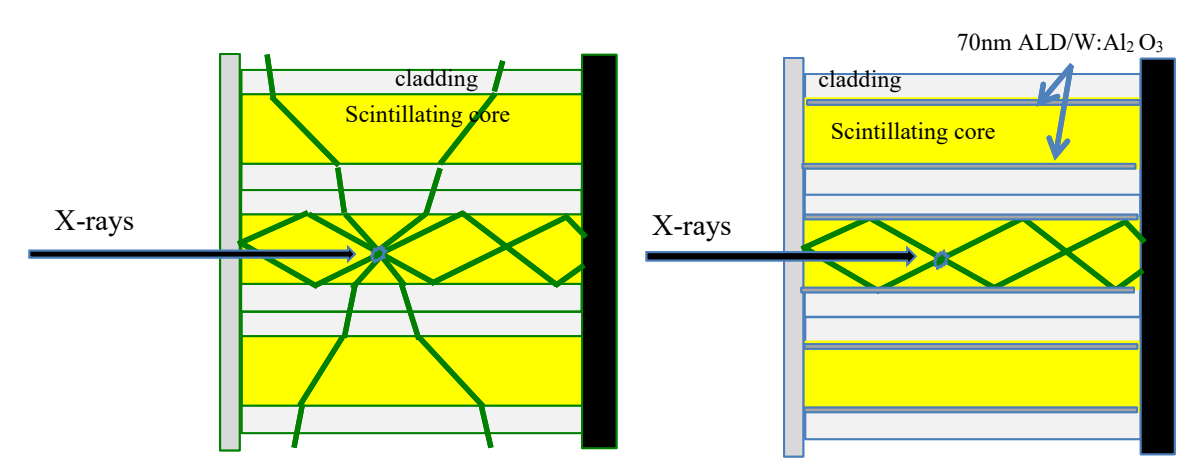


Fig. 5. Improvement of total internal reflection after deposition of ALD/W:Al₂O₃ coating, 70nm

2.3 Infiltrating the Bismuth Polymer into the Capillaries

A nitrogen pressurization chamber was built in order to infiltrate the bismuth-scintillating polymer uniformly through the pores of the optical channel plate. Before applying pressurization, the bismuth polymer was applied on top of the channel plate. Then pressurized nitrogen gas up to 400 psi was applied above the coherent disk while the bottom of the disk was held at atmospheric pressure. This pressure differential resulted in a uniform infiltration of the bismuth polymer into the capillaries. A semi rigid Teflon plate was used to secure the bottom of the pressure apparatus in order to insure that the channel plate would not crack from uneven compressive forces over the disk area.

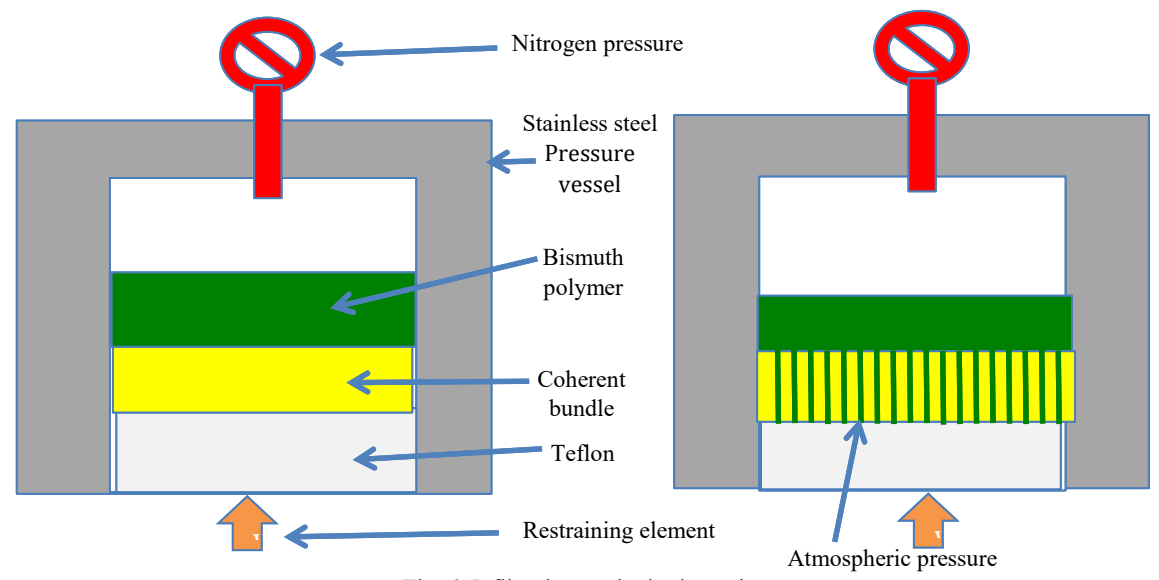


Fig. 6. Infiltration method schematic

Figure 6. demonstrates a schematic view of the nitrogen pressurization chamber and the manner in which the channel plate was secured and a pressure differential was established. A coherent disk infiltrated with the scintillating bismuth polymer is shown in Fig. 7 and 8.



Fig. 7. 2cm x 2cm x 1 mm (5 micron) Incom/bismuth polymer. A 2cm x 2cm plate has more than 20,000,000 capillaries.

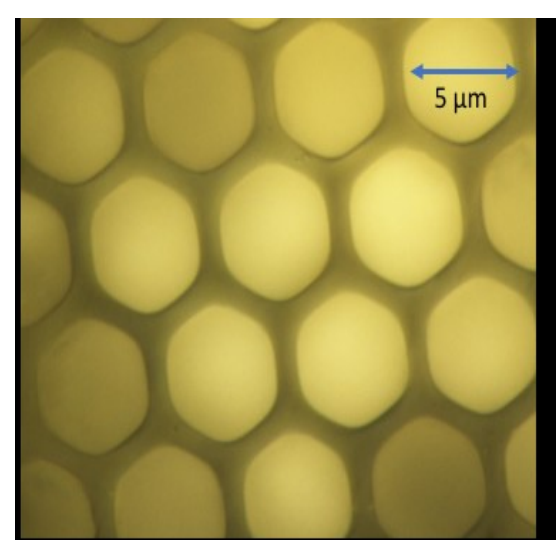


Fig. 8. Magnified view of bismuth polymer pressed uniformly into the 5 micron capillaries.

3. RESULTS

3.1 Demonstration of high resolution

A "Phantom" (from Metrigraphics LLC) was used to serve as a reference edge and calibrate the resolution. Two separate experiments were conducted using 265nm UV light in the first case and 50keV X-rays in the second case. The illuminated samples were 1 mm thick ALD/W:Al₂O₃ coated, bismuth polymer infiltrated optical channel plates. The 265nm UV sample had a pore size of 15 microns while the X-ray sample had a pore size of 10 microns. The image capture of the 265nm UV tests was done using a Nikon-D camera. The image capture of the 50keV X-ray tests was done using a SBIG STR-8300 cooled Monochrome CCD telescope camera.

Figure 9 shows the scintillated light images of the phantom recorded by the respective cameras. The left images are from the UV laser source and the right images are from the X-ray source.

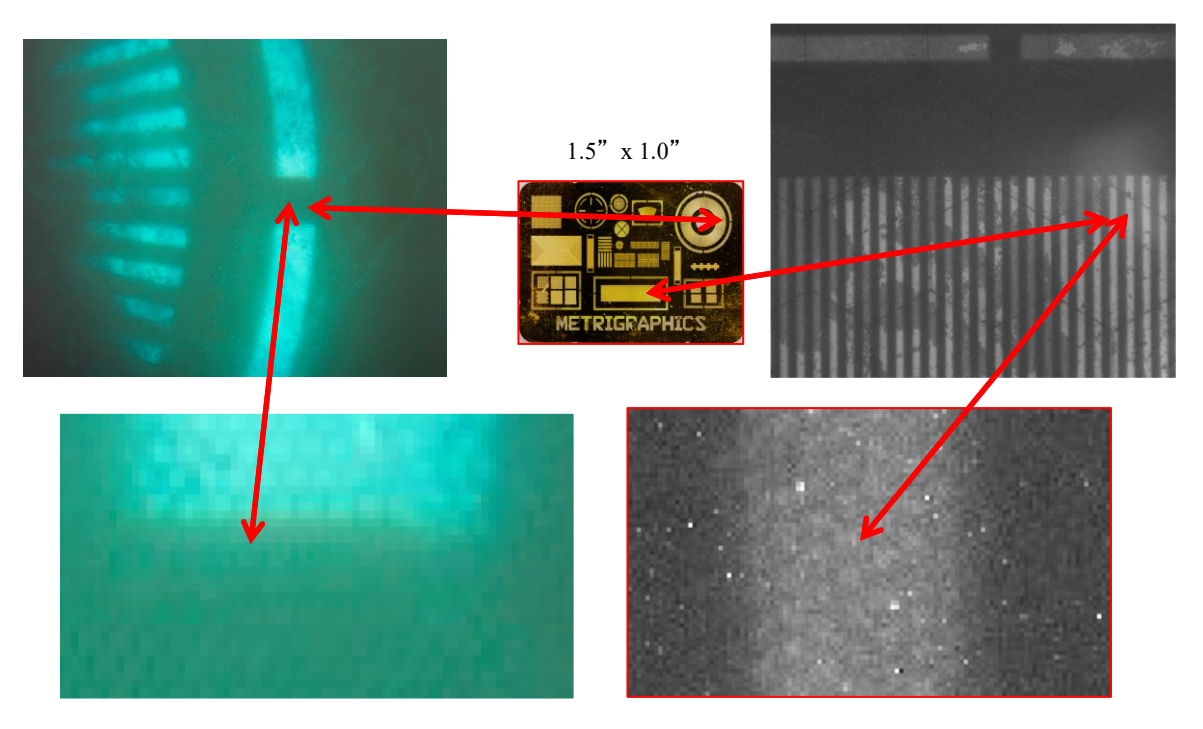


Fig. 9. Phantom: on the left, 15-micron pores; 265nm laser light; on the right, 10-micron pores, 50 keV X-rays.

3.2 Edge Shape Function, Line Shape Function, and Modulation Transfer Function (MTF)

UV light and X-rays with wavelengths less than or equal to 265nm have sufficient energy to excite electrons into the conduction band of the bismuth polymer and cause scintillation to occur. An approximation of the Modulation Transfer Function (MTF) for the bismuth polymer infiltrated glass optical channel system was done using the edge method. Here we explain the method used to estimate the MTF. An edge was identified from the 'Phantom' in an exposed and captured image and rotated to make it horizontal. A smaller region was subsequently cropped out, leaving equal numbers of pixels on either side of the edge. The sum of the pixel intensities along each row perpendicular to the edge was taken. Given that the line spread function of the raw data intensity values takes the form of a Gaussian distribution for an edge, a natural analytical model for the edge spread function can take the form of an error function. In equation 1 we propose an analytical model of the edge spread function and fit this model to the edge spread data. Equation 1 was fit to the edge spread data to generate the best fit parameters. F_{max} and F_{min} both refer to the maximum and minimum intensities of the raw data respectively. Using the fit parameters, we compare the resultant analytical line spread function which comes from the differentiated edge spread function and see that the model has good agreement with the line spread data. Examples of this comparison is done for UV light and X-rays in Figures 14-19.

$$ESF = \frac{F_{max} - F_{min}}{2} \left[Erf\left(\frac{x}{d}\right) + 1 \right] + \frac{Fmin}{2}$$
 (1)

The empirical Line Spread Function data was determined by the differences in intensities between rows, divided by the physical length represented by a pixel size. A zero padded Fast Fourier Transform of this line spread function was taken to produce the smoothed modulation transfer function.¹²

3.3 UV (265nm Laser) Exposure of the Coherent Bundle/Phantom

In Fig. 10, we see the corresponding Edge Spread Function (ESF), Line Spread Function (LSF) and Modulation Transfer Function (MTF) of the optical channel\Phantom exposed under a 265nm UV laser. The edge method was used to obtain the empirical data and the analytical model presented in equation 1 was fit to the data. An uneven distribution in the cores is believed to cause the scattering in the Line Shape Function.

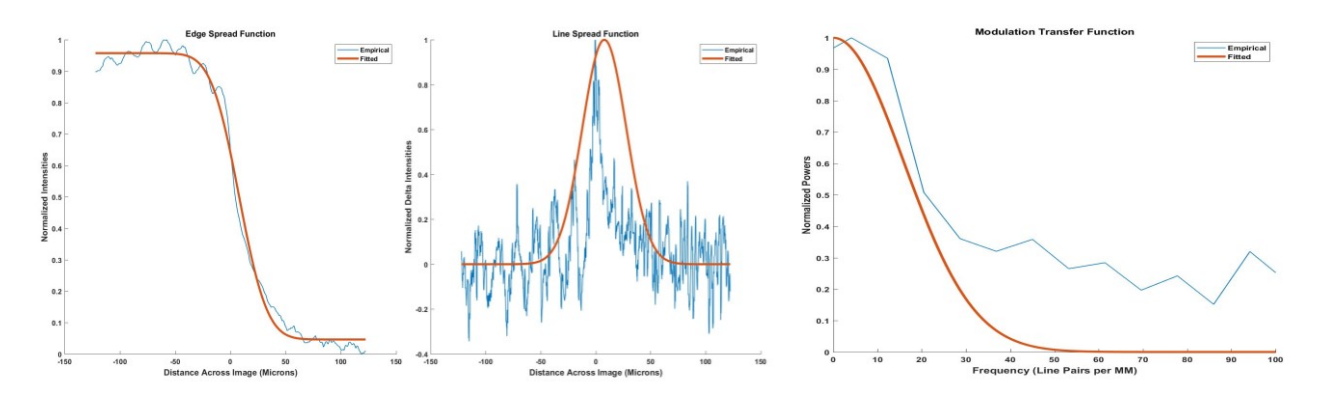


Fig. 10. UV 265nm Laser Exposure: Left: Edge Spread Function, Middle: Line Spread Function, Right: Modulation
Transfer Function

3.4 X-ray of the Coherent Bundle/Phantom

In Fig. 11, we see the corresponding Edge Spread Function (ESF), Line Spread Function (LSF) and Modulation Transfer Function (MTF) of the optical channel\Phantom exposed under a 50keV X-ray source. The edge method was used to obtain the empirical data and the analytical model presented in equation 1 was fit to the data. The analytical function has a good fit with the empirical data.

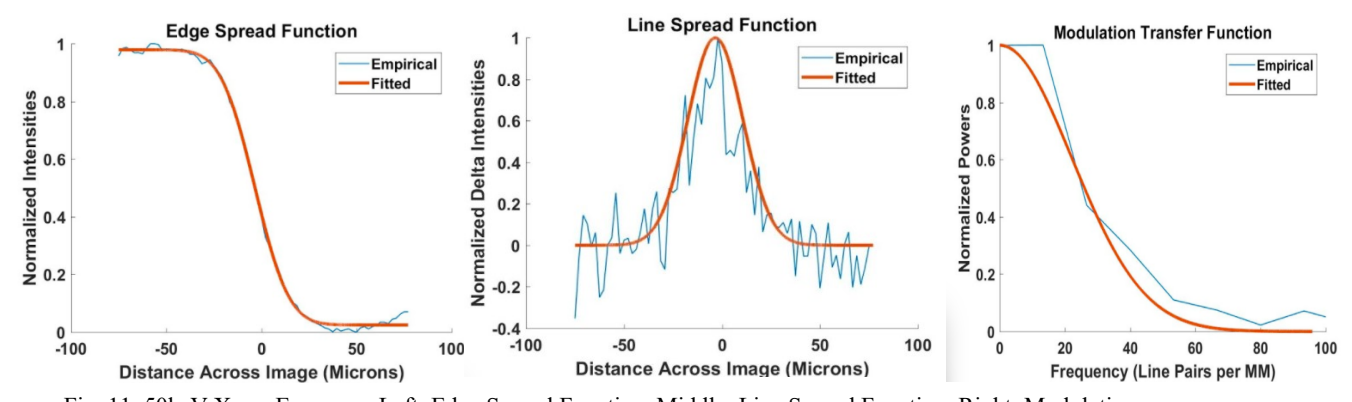


Fig. 11. 50keV X-ray Exposure: Left: Edge Spread Function, Middle: Line Spread Function, Right: Modulation
Transfer Function

From the MTF we estimate the resolution. The MTF at 10% of the normalized contrast is the standard definition for the visibility criterion, and corresponds to 50 line-pairs/mm, or 10 microns for the 50keV X-ray test. This demonstrates that the coherent disk pore size has set the image resolution in this experiment. Our future work will explore

While we have used different optical plate disks for the UV (15 microns, 265 laser, Fig. 10) and the X-ray (10 microns, 50keV, Fig. 11). It does provide a means of comparison with regard to the resolution

between the two: UV laser radiation, and X-rays. UV and X-rays produce the same type of scintillation in the bismuth-scintillating polymer, and the UV and X-rays may be compared with regard to the resolution.

3.5 Resolution and X-ray Dosage:

These results show that the pore size in optical channel plates can be used to set X-ray detection resolution as low as 10 microns. An equally important issue in X-ray imaging is reducing the necessary X-ray dose for proper exposure. In the case of optical channel plates, it is not only the pore size but also the internal reflection conditions that play a critical role in confining scintillated photons. The deposition of ALD/W:Al₂O₃ (10% W) (Atomic Layer Deposition: 70nm thick) on the pore sidewalls improved the critical angle of incidence for total internal reflection. In order to improve the Trapping Efficiency, it is important to find a cladding material with a lower index of refraction compared to that of the core. The Trapping Efficiency is a product of the planar rays and the skew rays.

$$TE = 1 - \left(\frac{n_{clad}}{n_{core}}\right)^2 \tag{2}$$

The refractive index of the cladding (borosilicate glass) is 1.45, and the refractive index of the core (scintillating bismuth polymer) is 1.7. The Trapping Efficiency, according to Eq. 1, is 0.27. The X-rays in Fig. 9 were taken at 600 seconds, which was enough to establish the principle of this device. However, it is critical to improve the Trapping Efficiency for medical X-ray imaging applications. We propose to use silver as a cladding material because it has a very low refractive index of 0.05 at the scintillation frequency of 500nm.

4. CONCLUSIONS

We have successfully filled infiltrated a scintillating bismuth polymer uniformly into 10 micron pore optical channel plates produced by Incom, Inc. This process can be scaled up to a large area. Initial cladding optimization experiments were conducted which demonstrated that a cladding of ALD/W:Al₂O₃ dramatically reduced signal crosstalk between pores. The reflectivity of the ALD/W:Al₂O₃ was only about 8%, yet it produced resolutions as good as 10 microns (50lp/mm), and we hope to achieve 5 micron resolution (100lp/mm) with optical channel plates with smaller pore sizes. We are presently experimenting with a silver cladding and expect to see one to two orders of magnitude improvement in reducing the exposure times to achieve comparable high-resolution images.

References

- [1] Nagarkar, V. V., et al. "Structured CsI (Tl) scintillators for X-ray imaging applications." *IEEE transactions on nuclear science*45.3 (1998): 492-496.
- [2] Yakunin, Sergii, et al. "Detection of X-ray photons by solution-processed lead halide perovskites." *Nature photonics* 9.7 (2015): 444.
- [3] Sahlholm, Anna, Olof Svenonius, and Sture Petersson. "Scintillator technology for enhanced resolution and contrast in X-ray imaging." *Nuclear Instruments and Methods in Physics Research Section A: Accelerators, Spectrometers, Detectors and Associated Equipment* 648 (2011): S16-S19.
- [4] Hormozan, Yashar, Ilya Sychugov, and Jan Linnros. "High-resolution x-ray imaging using a structured scintillator." *Medical physics* 43.2 (2016): 696-701.
- [5] T.F. Morse, et al., Method and Apparatus for Creating Coherent Bundle of Scintillating Fibers, USP9611168, July 2017.
- [6] T.F. Morse, et al., High definition scintillation detector for medicine, homeland Security, and non-destructive evaluation, 20120101374, June 2013.
- [7] Cherepy, N. J., et al. "Bismuth-loaded plastic scintillators for gamma spectroscopy and neutron active interrogation." *Nuclear Science Symposium and Medical Imaging Conference (NSS/MIC)*, 2012 IEEE. IEEE, 2012.
- [8] Cherepy, Nerine J., et al. "Bismuth-and lithium-loaded plastic scintillators for gamma and neutron detection." *Nuclear Instruments and Methods in Physics Research Section A: Accelerators, Spectrometers, Detectors and Associated Equipment* 778 (2015): 126-132.

- [9] Rupert, B. L., et al. "Bismuth-loaded plastic scintillators for gamma-ray spectroscopy." *EPL (Europhysics Letters)* 97.2 (2012): 22002.
- [10] NIST X-Ray Attenuation, Web.
- [11] Babar, Shaista, et al. "W: Al2O3 nanocomposite thin films with tunable optical properties prepared by atomic layer deposition." *The Journal of Physical Chemistry C* 120.27 (2016): 14681-14689.
- [12] Buhr, Egbert, Susanne Günther-Kohfahl, and Ulrich Neitzel. "Simple method for modulation transfer function determination of digital imaging detectors from edge images." *Medical Imaging 2003: Physics of Medical Imaging*. Vol. 5030. International Society for Optics and Photonics, 2003.